PAPER

A fluorescent acrylamide-type monomer bearing an environment-sensitive methoxybenzocoumarin structure for the development of functional polymeric sensors†

Seiichi Uchiyama,*[a] Patricia Remón,[a,b] Uwe Pischel,[b] Kyoko Kawamoto[a] and Chie Gota[a]

A new fluorescent acrylamide-type monomer bearing a hydrogen bonding- and polarity-sensitive benzo-coumarin fluorophore was synthesized. The absorption spectra, fluorescence spectra, and fluorescence lifetime of a model compound were measured in ten solvents with different hydrogen-bonding abilities and polarities to investigate the sensitivity of the fluorophore to the surrounding environment. These spectroscopic studies demonstrated that the fluorophore emits stronger fluorescence in more protic, polar environments. A fluorescent polymeric thermometer was prepared from *N*-isopropylacrylamide and the new fluorescent monomer, and it showed good functionality in aqueous solution (*e.g.*, high sensitivity to temperature changes and high chemical stability), indicating the applicability of the herein developed fluorescent monomer for use in functional sensors.

Introduction

Environment-sensitive fluorophores change their photophysical properties (*e.g.*, fluorescence quantum yield, maximum emission wavelength, and fluorescence lifetime) depending on the surrounding environment. Fluorescent monomers consisting of an environment-sensitive fluorophore and a polymerizable vinyl bond are valuable in polymer chemistry because they can facilitate the elucidation of the microenvironments of macromolecules[1] and the development of functional polymeric materials with applications in a wide range of scientific disciplines.[2] Examples of the latter case include fluorescent monomers bearing an environment-sensitive dansyl,[3] benzofurazan,[4–6] aminocoumarin,[7] or naphthalimide[8] fluorophore, which have been used to construct fluorescent polymeric thermometers by us and other groups. Intracellular thermometry can now be performed with these fluorescent polymeric thermometers.[6,9] Fluorescent polymeric sensors for potassium ions,[10] sulfate ions,[11] phosphatidylinositol-4,5-bisphosphate,[12] and phosphatidylserine[13] are also examples of macromolecular materials created from fluorescent monomers containing an environment-sensitive fluorophore. The use of some of these sensors[12,13] has been explored to monitor biologically important molecules in live cell imaging. It should be noted that all of the fluorescent monomers in the functional polymers described above bear an environment-sensitive fluorophore, which shows stronger fluorescence in less protic, polar environments (*e.g.*, in an aprotic organic solvent, such as ethyl acetate). Fluorescent monomers containing a fluorophore with the opposite sensitivity to the environment, *i.e.*, those that emit stronger fluorescence in more protic, polar environments, are worthwhile components for the development of functional polymers with new properties.

In our previous study,[14] we found that 8-methoxy-4-methyl-2*H*-benzo[*g*]chromen-2-one (**MBC**) (Fig. 1) is an environment-sensitive fluorophore that emits stronger fluorescence in more protic, polar environments. The unique fluorescent monomer (8-methoxy-2-oxo-2*H*-benzo[*g*]chromen-4-yl)methyl acrylate (**MBC-AE**), which bears the **MBC** structure, was synthesized, and a fluorescent polymeric thermometer, poly(*N*-isopropylacrylamide-*co*-MBC-AE) (poly(NIPAM-*co*-MBC-AE)) was prepared as an example of the use of this monomer. Poly(NIPAM-*co*-MBC-AE) showed temperature-dependent fluorescence in aqueous solution because the microenvironment near the **MBC-AE** units was changed by the thermo-responsive behavior of the polyNIPAM units.[15] Nevertheless, the repeatable thermo-responsive function of poly(NIPAM-*co*-MBC-AE) was observed only under acidic conditions because the **MBC-AE** units in poly(NIPAM-*co*-MBC-AE) were hydrolyzed under neutral and basic conditions.

[a]*Graduate School of Pharmaceutical Science, The University of Tokyo, 7-3-1 Hongo Bunkyo-ku, Tokyo 113-0033, Japan. E-mail: seiichi@mol.f.u-tokyo.ac.jp*
[b]*CIQSO-Centre for Research in Sustainable Chemistry and Department of Chemistry, University of Huelva, Campus de El Carmen s/n, E-21071 Huelva, Spain*
†Electronic supplementary information (ESI) available: Table S1 and Fig. S1, S2. See DOI: 10.1039/c6pp00150e
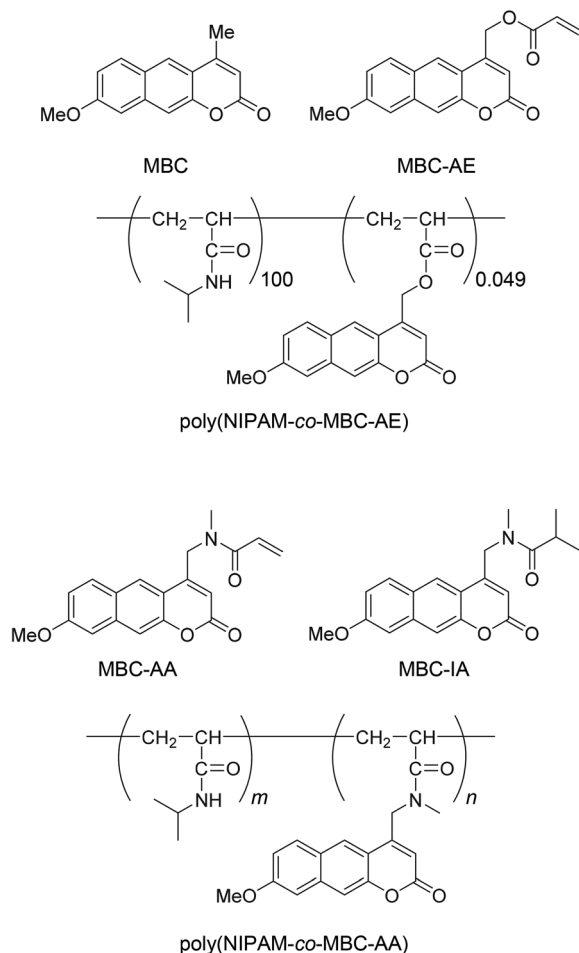
This journal is © The Royal Society of Chemistry and Owner Societies 2016

Photochem. Photobiol. Sci., 2016, **15**, 1239–1246 | **1239**

Fig. 1 Chemical structures of **MBC**, **MBC-AE**, poly(NIPAM-*co*-MBC-AE), **MBC-AA**, **MBC-IA**, and poly(NIPAM-*co*-MBC-AA).

To address this shortcoming, herein, we synthesized *N*-((8-methoxy-2-oxo-2*H*-benzo[*g*]chromen-4-yl)methyl)-*N*-methyl-acrylamide (**MBC-AA**) as a new acrylamide-type fluorescent monomer. The amide-type **MBC-AA** unit was expected to be more tolerant to hydrolysis than the ester-type **MBC-AE** unit when introduced into a polymer. *N*-((8-Methoxy-2-oxo-2*H*-benzo[*g*]chromen-4-yl)methyl)-*N*-methylisobutylamide (**MBC-IA**) was also synthesized as a model compound of the **MBC-AA** unit. The fluorescence properties of **MBC-IA** were investigated in ten solvents to determine the sensitivity of the fluorophore to the surrounding environment. In addition, poly(NIPAM-*co*-MBC-AA) was prepared, and its fluorescence properties were studied. The utility of the new fluorescent monomer **MBC-AA** was assessed by investigating the thermo-responsive function of poly(NIPAM-*co*-MBC-AA) in water.

Experimental

Materials and apparatus

Poly(NIPAM-*co*-MBC-AE) (weight-average molecular weight M_w = 148 000, number-average molecular weight M_n = 51 500,

M_w/M_n = 2.87) was obtained as previously reported.[14] ^{1}H NMR spectra were recorded using a Bruker Avance 400 spectrometer. The mass spectra acquired *via* electrospray ionization (ESI) were recorded using a Bruker micrOTOF-05 spectrometer. The melting points were measured using a Round Science RFS-10 and are uncorrected. The gel-permeation chromatography (GPC) equipment consisted of a JASCO PU-2080 pump, a JASCO RI-2031 refractive index detector, a JASCO FP-2020 fluorescence detector, a JASCO CO-2060 column thermostat, and a Shodex GPC KD-806 M column. A calibration curve was obtained using polystyrene standards, and 1-methyl-2-pyrrolidinone containing LiBr (5 mM) was used as the eluent.

Synthesis

8-Methoxy-4-((methylamino)methyl)-2*H*-benzo[*g*]chromen-2-one (MBC-MA). 4-Chloromethyl-8-methoxy-2*H*-benzo[*g*]chromen-2-one (100 mg, 0.36 mmol)[14] was dissolved in acetonitrile (20 mL). After the addition of 40% methylamine solution (607 μL, 7.0 mmol), the mixture was stirred at 50 °C for 3 h. Then, the reaction mixture was evaporated to dryness under reduced pressure, and the residue was separated by chromatography on silica gel using dichloromethane–methanol (95 : 5, v/v) to afford **MBC-MA** (21.2 mg, 22%) as a pale yellow powder: mp, 132–133 °C; ^{1}H NMR (CDCl₃) δ 8.01 (1H, s), 7.76 (1H, d, *J* = 9.0 Hz), 7.51 (1H, s), 7.11 (1H, dd, *J* = 9.0, 2.2 Hz), 7.03 (1H, d, *J* = 2.2 Hz), 6.48 (1H, s), 4.00 (2H, s), 3.93 (3H, s), 2.58 (3H, s); ^{13}C NMR (CDCl₃) δ 161.8, 160.2, 153.6, 151.7, 136.9, 130.8, 126.2, 124.6, 120.1, 117.0, 113.6, 112.4, 105.1, 56.0, 52.2, 37.1. High-resolution ESI mass spectrometry (HR-ESI-MS): *m/z* Calcd for $C_{16}H_{16}NO_3^+$ [M + H]⁺ 270.1125. Found 270.1125.

MBC-AA. **MBC-MA** (70 mg, 0.26 mmol) was dissolved in acetonitrile (10 mL). After the addition of triethylamine (36.2 μL, 0.26 mmol) and acryloyl chloride (82.2 μL, 1.02 mmol), the mixture was stirred at 50 °C for 4.5 h. Then, Na₂CO₃ (1 g) was added to the solution to stop the reaction. After filtration to remove excess Na₂CO₃, the reaction mixture was evaporated to dryness under reduced pressure, and the residue was chromatographed on silica gel using dichloromethane–methanol (50 : 1, v/v) to afford **MBC-AA** (60.9 mg, 72%) as a yellow powder: mp, 166–167 °C; ^{1}H NMR (CDCl₃) δ 8.04, 7.91 (1H, s), 7.77 (1H, d, *J* = 9.2 Hz), 7.58, 7.55 (1H, s), 7.11–7.18 (1H, m), 7.07 (1H, s), 6.43–6.73 (2H, m), 6.24, 6.17 (1H, s), 5.69–5.84 (1H, m), 4.91, 4.87 (2H, s), 3.94 (3H, s), 3.16 (3H, s); ^{13}C NMR (CDCl₃) δ 166.7, 160.6, 159.7, 150.7, 150.0, 136.4, 130.3, 130.0, 129.5, 126.7, 125.5, 124.2, 123.0, 119.9, 119.5, 115.5, 112.6, 112.0, 111.7, 104.5, 55.4, 53.4, 50.1, 48.0, 35.7, 35.0, 29.6, 23.3. HR-ESI-MS: *m/z* Calcd for $C_{19}H_{17}NNaO_4^+$ [M + Na]⁺ 346.1050. Found 346.1055.

MBC-IA. **MBC-MA** (20 mg, 0.074 mmol) was dissolved in acetonitrile (3 mL). After the addition of triethylamine (13.5 μL, 0.097 mmol) and isobutyric anhydride (16.1 μL, 0.097 mmol), the mixture was stirred at room temperature for 4 h. Then K₂CO₃ (1 g) was added to the solution to stop the reaction. After filtration to remove excess K₂CO₃, the reaction

1240 | *Photochem. Photobiol. Sci.*, 2016, **15**, 1239–1246

This journal is © The Royal Society of Chemistry and Owner Societies 2016

mixture was evaporated to dryness under reduced pressure, and the residue was chromatographed on silica gel using dichloromethane–methanol (50 : 1, v/v) to afford **MBC-IA** (19.3 mg, 77%) as a yellow powder: mp, 188–190 °C; ^{1}H NMR (CDCl$_3$) δ 8.05, 7.93 (1H, s), 7.76–7.81 (1H, m), 7.64, 7.59 (1H, s), 7.09–7.18 (2H, m), 6.22, 6.17 (1H, s), 4.87, 4.84 (2H, s), 3.98, 3.95 (3H, s), 3.11, 3.09 (3H, s), 2.61–2.97 (m, 1H), 1.17–1.22 (6H, m); ^{13}C NMR (CDCl$_3$) δ 177.4, 160.8, 159.7, 150.9, 150.7, 136.5, 130.4, 125.6, 124.5, 119.6, 115.7, 113.1, 111.8, 104.5, 55.4, 47.9, 35.2, 30.5, 29.7, 19.2. HR-ESI-MS: m/z Calcd for C$_{20}$H$_{21}$NNaO$_4^+$ [M + Na]$^+$ 362.1363. Found 362.1368.

Poly(NIPAM-*co*-MBC-AA). NIPAM (2.5 mmol), **MBC-AA** (2.5 µmol), and α,α′-azobisisobutyronitrile (25 µmol) were dissolved in 1,4-dioxane (5 mL), and the solution was bubbled with dry Ar for 30 min to remove dissolved oxygen. The solution was heated at 60 °C for 6 h and then cooled to room temperature. The reaction mixture was then poured into diethyl ether (200 mL). The resulting polymer was collected by filtration and purified by reprecipitation using 1,4-dioxane (5 mL)–diethyl ether (100 mL) (yield: 76%). The proportion of the **MBC-AA** unit in the copolymer was determined by comparing the absorbance in methanol with that of the model fluorophore **MBC-IA**. The molecular weights (M_w and M_n) were determined by GPC with a refractive index detector.

Photophysical studies of MBC-IA

UV/Vis absorption spectra (10 or 30 µM) were recorded at 25 °C using a JASCO V-550 UV/Vis spectrophotometer. Fluorescence spectra (10 µM) were recorded using a JASCO FP-8500 spectrofluorimeter with a Hamamatsu R928 optional photomultiplier tube (operative range: 200–850 nm) at 25 °C and were corrected using a JASCO ESC-333 substandard light source. The fluorescence quantum yield of **MBC-IA** in ethanol (Φ_f = 0.26) was determined using a JASCO ILF-835 integrating sphere unit.[6e] The fluorescence quantum yields in other solvents were determined from eqn (1), where F is the area under the corrected fluorescence spectrum obtained with excitation at 345 nm, A is the absorbance at 345 nm, n is the refractive index of the solvent, and the subscripts R and S indicate the reference (*i.e.*, **MBC-IA** in ethanol) and the sample, respectively.

$$\Phi_{f,s} = \Phi_{f,R} F_S A_R n_S^2 / F_R A_S n_R^2 \tag{1}$$

The fluorescence lifetimes (τ_f) were determined using a time-correlated single-photon counting (TCSPC) fluorimeter Horiba Jobin Yvon FluoroCube 3000U at 25 °C. The samples were excited with a Horiba NanoLED-370 (excitation: 370 nm) at a repetition rate of 1 MHz. The recorded fluorescence decay curves ($I(t)$) were fitted by an exponential function expressed as eqn (2), where B is the pre-exponential factor, and t is the time.

$$I(t) = \sum_{i=1}^{n} B_i \exp\left(-\frac{t}{\tau_i}\right) \tag{2}$$

Then, the τ_f values were calculated using eqn (3).

$$\tau_f = \sum_{i=1}^{n} B_i \tau_i^2 / \sum_{i=1}^{n} B_i \tau_i \tag{3}$$

The fractional contributions (P_i for τ_i) were calculated using eqn (4).

$$P_i = 100 \times B_i \tau_i / \sum_{i=1}^{n} B_i \tau_i \tag{4}$$

According to the fluorescence lifetime and the fluorescence quantum yield, the fluorescence rate constant (k_f) and non-radiative rate constant (k_{nr}) were calculated using eqn (5) and (6), respectively.

$$k_f = \frac{\Phi_f}{\tau_f} \tag{5}$$

$$k_{nr} = \frac{1 - \Phi_f}{\tau_f} \tag{6}$$

Functional studies of poly(NIPAM-*co*-MBC-AA)

The fluorescence spectra of poly(NIPAM-*co*-MBC-AA) (0.01% w/v) were recorded in 1,4-dioxane, acetonitrile, ethanol, methanol, and water with excitation at 345 nm. After ten cycles of heating (to 45 °C) and cooling (to 25 °C) in water, the polymer solution was lyophilized, and the residue was re-dissolved in 1-methyl-2-pyrrolidinone (0.5% w/v) for subsequent GPC. The hydrodynamic diameter of poly(NIPAM-*co*-MBC-AA) was estimated from dynamic light scattering (DLS) measurements using a Zetasizer Nano ZS (Malvern Instruments). The samples (0.01% w/v) were equilibrated at 20 °C for 10 min.

Results and discussion

Synthesis of MBC-AA and MBC-IA

The new fluorescent monomer **MBC-AA** and the model compound **MBC-IA** were synthesized from 4-chloromethyl-8-methoxy-2*H*-benzo[*g*]chromen-2-one[14] by two-step reactions (Fig. 2). In the first reaction, the methylamino group was introduced by nucleophilic substitution under mild conditions.
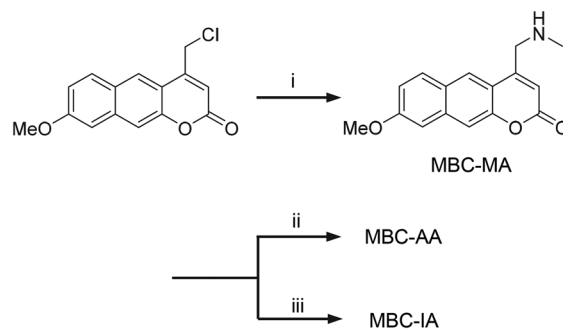

Fig. 2 Synthesis of **MBC-AA** and **MBC-IA**. (i) 40% MeNH$_2$, MeCN, 50 °C, 3 h (22%); (ii) acryloyl chloride, Et$_3$N, MeCN, 50 °C, 4.5 h (72%); and (iii) isobutyric anhydride, Et$_3$N, MeCN, rt, 4 h (77%).

This journal is © The Royal Society of Chemistry and Owner Societies 2016

Photochem. Photobiol. Sci., 2016, **15**, 1239–1246 | **1241**

Then, acylation was performed using acryloyl chloride and iso-butyric anhydride to obtain **MBC-AA** and **MBC-IA**, respectively.

Fluorescence properties of MBC-IA

The absorption and fluorescence spectra of the model fluorophore **MBC-IA** were recorded in ten solvents (*n*-hexane, 1,4-dioxane, ethyl acetate, acetonitrile, chloroform, ethanol, methanol, a mixture of water and methanol [4 : 1, v/v], water, and trifluoroethanol) (Fig. 3). Table 1 summarizes the photophysical properties of **MBC-IA** in these solvents and the solvents' hydrogen-bonding ability (*i.e.*, hydrogen-bond donor acidity α (ref. 16)) and polarity (*i.e.*, dielectric constant D (ref. 17)). Similar to **MBC**,[14] although **MBC-IA** was almost non-fluorescent in aprotic, apolar solvents (*e.g.*, $\Phi_f = 0.0054$ in *n*-hexane), it strongly fluoresced in protic, polar solvents (*e.g.*, $\Phi_f = 0.35$ in methanol).

Regarding the maximum emission wavelength, **MBC-IA** fluoresced at longer wavelengths as the hydrogen-bonding ability and polarity of the solvent increased, indicating that the first singlet state of **MBC-IA** has an intramolecular charge transfer (ICT) character.[18] Table 1 also shows the fluorescence lifetimes (see Fig. S1† for the original fluorescence decay curves), fluorescence rate constants, and non-radiative rate constants of **MBC-IA** in the different solvents. The high efficiency of the non-radiative relaxation process in **MBC-IA** in aprotic, apolar solvents is because of the proximity of an emissive $\pi\pi^*$ state to a non-emissive $n\pi^*$ state.[19] Comparing the photophysical properties of **MBC-IA** in acetonitrile ($\Phi_f = 0.031$, hydrogen-bond donor acidity $\alpha = 0.19$ and dielectric constant $D = 37.5$) and in methanol ($\Phi_f = 0.35$, $\alpha = 0.93$, and $D = 32.6$) revealed that the fluorescence process of **MBC-IA** is dominantly influenced by the hydrogen-bonding ability of the solvent rather than by its polarity. The non-radiative process of **MBC-IA** in water was accelerated compared to that in methanol, although water has a stronger hydrogen-bonding ability ($\alpha = 1.17$) than methanol ($\alpha = 0.93$). The proximity of the first singlet $\pi\pi^*$ state to the ground state in more polar environments, as indicated by the longer emission wavelength (*i.e.*, 540 nm in water), increases the efficiency of the non-radiative internal conversion. This effect has been established as the "energy gap law"[20] in photochemistry. It should be also noted that the fluorescence rate constant of **MBC-IA** was strongly influenced by the solvents (see Table 1). Because such a decrease in the k_f value in the non-polar solvents (*i.e.*, *n*-hexane, 1,4-dioxane and ethyl acetate) was not observed in the original fluorophore **MBC**,[19] the dependency of the k_f
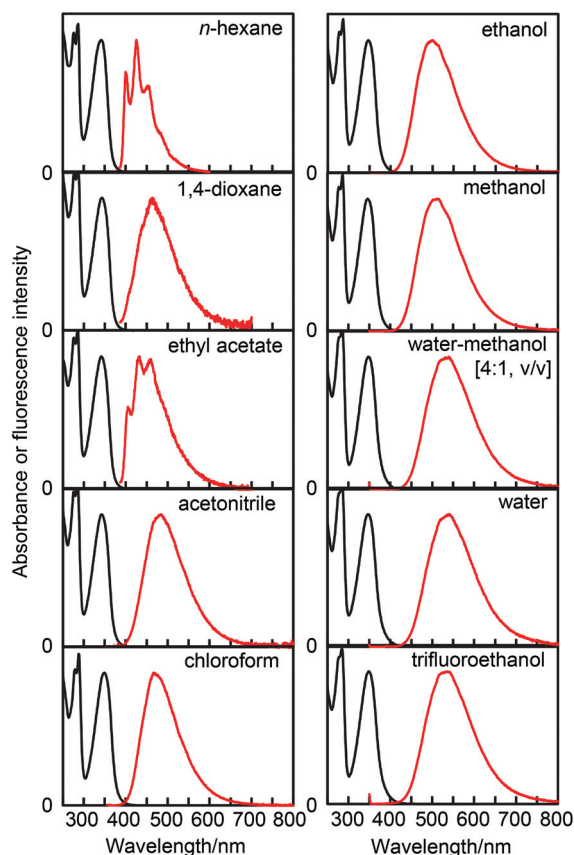

Fig. 3 Absorption (black line) and fluorescence (red line) spectra of **MBC-IA** (10 μM) in various solvents at 25 °C. All fluorescence spectra were recorded with excitation at the maximum absorption wavelength.

Table 1 Photophysical properties of **MBC-IA**: fluorescence quantum yield (Φ_f), maximum absorption wavelength (λ_{abs}), molar absorption coefficient (ε), maximum emission wavelength (λ_{em}), fluorescence lifetime (τ_f), fluorescence rate constant (k_f), and non-radiative rate constant (k_{nr})

Solvent	α^a	D^b	Φ_f	λ_{abs}/nm	ε/M^{-1} cm^{-1}	λ_{em}/nm	τ_f/ns	$k_f/10^7$ s^{-1}	$k_{nr}/10^7$ s^{-1}
n-Hexane	0.00	1.9	0.0054	342	16 100	425	0.98	0.55	100
1,4-Dioxane	0.00	2.2	0.0033	343	16 300	462	0.86^c	0.38	116
Ethyl acetate	0.00	6.0	0.0053	342	15 500	432	1.1	0.47	87
Acetonitrile	0.19	37.5	0.031	343	15 200	483	2.7^d	1.1	35
Chloroform	0.44	4.8	0.052	349	16 400	468	3.0^e	1.7	32
Ethanol	0.83	24.3	0.26	347	15 600	500	5.2	4.9	14
Methanol	0.93	32.6	0.35	346	14 900	512	6.3	5.5	10
Water–methanol [4 : 1, v/v]		70.7	0.28	348	14 400	540	4.4	6.3	16
Water	1.17	78.5	0.17	346	13 100	540	3.4	5.1	24
Trifluoroethanol	1.51	26.8	0.33	349	15 600	538	6.0	5.4	11

^{a} Hydrogen-bond donor acidity of the solvent.[16] ^{b} Dielectric constant of the solvent.[17] ^{c} Average fluorescence lifetime of three components: $\tau_1 = 0.21$ ns (45%), $\tau_2 = 1.1$ ns (51%), and $\tau_3 = 5.0$ ns (3.7%). ^{d} Average fluorescence lifetime of two components: $\tau_1 = 0.63$ ns (53%) and $\tau_2 = 5.1$ ns (47%). ^{e} Average fluorescence lifetime of two components: $\tau_1 = 1.2$ ns (69%) and $\tau_2 = 7.0$ ns (31%).
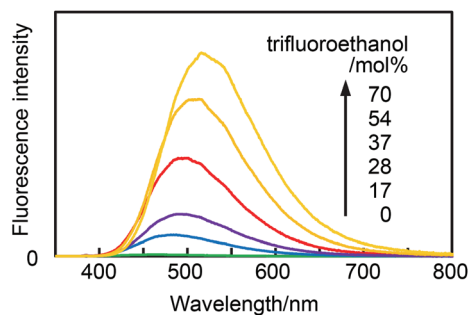
1242 | *Photochem. Photobiol. Sci.*, 2016, **15**, 1239–1246

This journal is © The Royal Society of Chemistry and Owner Societies 2016

Fig. 4 Fluorescence spectra of **MBC–IA** (10 μM) in a mixture of 1,4-dioxane and trifluoroethanol at 25 °C. All samples were excited at 345 nm.
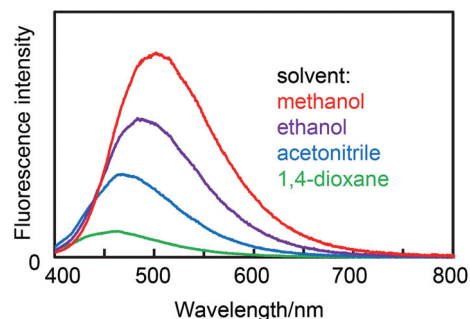

Fig. 5 Fluorescence spectra of poly(NIPAM–co–MBC-AA) in 1,4-dioxane, acetonitrile, ethanol, and methanol at 25 °C. All samples (0.01% w/v) were excited at 345 nm.

values of **MBC-IA** on the solvents can be ascribed to the interaction of the fluorophore (*i.e.*, the methoxybenzocoumarin moiety) with the side chain (*i.e.*, the methylisobutylamide moiety) in the non-polar solvents.

To further demonstrate the sensitivity of **MBC-IA** to the surrounding environment, its fluorescence spectra were obtained in mixtures of aprotic and apolar 1,4-dioxane (α = 0.00, and D = 2.2) and protic and polar trifluoroethanol (α = 1.51, and D = 26.8). As shown in Fig. 4, the fluorescence intensity of **MBC-IA** dramatically increased as the molar ratio of trifluoroethanol in the mixture increased. These results are in accordance with the general observation that **MBC-IA** emits more strongly in more protic, polar media.

Fluorescence properties of poly(NIPAM-co-MBC-AA)

Next, poly(NIPAM-co-MBC-AA) ($m : n$ = 100 : 0.06 in Fig. 1, M_w = 125 000, M_n = 41 000, and M_w/M_n = 3.04) was prepared by random copolymerization, and its fluorescence properties were investigated. First, the fluorescence spectra of poly(NIPAM-co-MBC-AA) were obtained in organic solvents (1,4-dioxane, acetonitrile, ethanol, and methanol). In these solvents, poly(NIPAM-co-MBC-AA) takes a flexible form, and the hydrodynamic diameters of poly(NIPAM-co-MBC-AA) at 20 °C were estimated by DLS measurements to be 10.35 ± 0.36, 8.00 ± 1.24, 15.95 ± 0.84, and 10.22 ± 1.70 nm in 1,4-dioxane, acetonitrile, ethanol, and methanol, respectively (Fig. S2†). As shown in Fig. 5, poly(NIPAM-co-MBC-AA) emitted stronger fluorescence at longer wavelengths in a more protic, polar solvent. Thus, the sensitivity of the methoxybenzocoumarin fluorophore (*i.e.*, **MBC**) to the surrounding environment was preserved, even when it was introduced into a polymer structure.

Finally, the fluorescence properties of poly(NIPAM-co-MBC-AA) in water (hydrodynamic diameter: 12.40 ± 1.55 nm at 20 °C, Fig. S2†) were evaluated by changing the temperature. Fig. 6a and b show the fluorescence responses of poly(NIPAM-co-MBC-AA) to increasing temperatures. This fluorescence behavior is attributable to change in the microenvironment of the NIPAM units that occurs at approximately 32 °C: solvent water molecules are repelled from the NIPAM units at temperatures higher than 32 °C.[15] As displayed in Fig. 6c, the

fluorescence response of poly(NIPAM-co-MBC-AA) to the temperature variation was highly reproducible over ten cycles of heating and cooling, whereas that of poly(NIPAM-co-MBC-AE) lacked stability and sensitivity. The difference in the functional reproducibility between poly(NIPAM-co-MBC-AA) and poly(NIPAM-co-MBC-AE) was attributed to the robustness of the fluorescent units. Aliquots of aqueous poly(NIPAM-co-MBC-AA) and poly(NIPAM-co-MBC-AE) after ten cycles of functional assessment (heating to 45 °C and cooling to 25 °C) were analyzed by GPC with a fluorescence detector. As indicated in Fig. 7, the **MBC-AA** units of poly(NIPAM-co-MBC-AA) remained unchanged during the heating and cooling cycles, whereas the **MBC-AE** units of poly(NIPAM-co-MBC-AE) decomposed significantly. The ester linkage of **MBC-AE** units was easily hydrolyzed, even in neutral aqueous solution. The fluorophore cleaved from poly(NIPAM-co-MBC-AE) was no longer sensitive to the heat-induced local environmental change near the NIPAM units, resulting in the deterioration of the function as seen in Fig. 6c. On the other hand, the new fluorescent monomer **MBC-AA** does not exhibit the low stability of the conventional monomer **MBC-AE**.

In the fluorescence response of poly(NIPAM-co-MBC-AA) in water (Fig. 6a), the maximum emission wavelength shifted from 520 to 470 nm as the temperature increased from 30 to 40 °C. This remarkable spectral shift enabled us to consider using poly(NIPAM-co-MBC-AA) as a ratiometric fluorescent thermometer. Fig. 6d shows the relationship between the fluorescence intensity ratio of poly(NIPAM-co-MBC-AA) at 470 and 520 nm (FI_{470}/FI_{520}) and the temperature. The FI_{470}/FI_{520} value was also highly reproducible over ten cycles of heating and cooling (Fig. 6e). Although the functional temperature range was relatively narrow, the average sensitivity of the fluorescence intensity ratio (FI_{470}/FI_{520}) of poly(NIPAM-co-MBC-AA) as the temperature varied from 32 to 38 °C was 15.0% °C^{-1}, which is much higher than those of the conventional ratiometric fluorescent thermometers functioning in water, such as fluorophore(s)-labeled thermo-responsive polymers (3.4–11.3% °C^{-1}),[4a,6e,21] fluorophore(s)- and/or lumophore(s)-containing polymer nanoparticles (2.0–4.2% °C^{-1}),[22] emissive inorganic nanoparticles (0.26–3.1% °C^{-1}),[23] a small organic

This journal is © The Royal Society of Chemistry and Owner Societies 2016

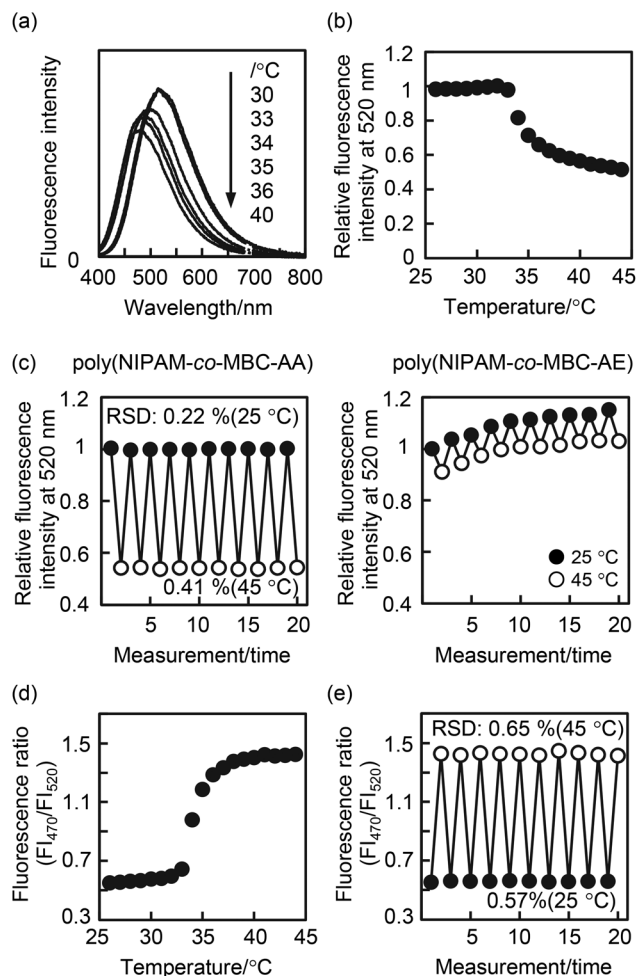*Photochem. Photobiol. Sci.*, 2016, **15**, 1239–1246 | **1243**

Fig. 6 Function of poly(NIPAM-*co*-MBC-AA) in water as a fluorescent polymeric thermometer. (a) Representative fluorescence spectra with increasing temperature. In the region indicated by dotted lines near 690 nm, scatter due to excitation light overlapped with the fluorescence spectra. (b) Change in the fluorescence intensity at 520 nm. Normalized at 25 °C. (c) Reversibility of the fluorescence intensities of poly(NIPAM-*co*-MBC-AA) (left) and a reference copolymer poly(NIPAM-*co*-MBC-AE) (right) over ten cycles of heating (45 °C, open circle) and cooling (25 °C, closed circle). (d) Change in the fluorescence intensity ratio at 470 nm and 520 nm (Fl$_{470}$/Fl$_{520}$). (e) Reversibility of the fluorescence ratio Fl$_{470}$/Fl$_{520}$ over ten cycles of heating (45 °C, open circle) and cooling (25 °C, closed circle). The data shown in (b)–(e) were obtained from the fluorescence spectra collected as the temperature increased. The relative standard deviations (RSDs) indicated in (c) and (e) were calculated from the fluorescence intensities at each temperature (n = 10). All samples (0.01% w/v) were excited at 345 nm.

Fig. 7 Stability of poly(NIPAM-*co*-MBC-AA) in water. Chromatograms of pristine poly(NIPAM-*co*-MBC-AA) (a) and poly(NIPAM-*co*-MBC-AE) (c), and the corresponding samples after ten cycles of heating (45 °C) and cooling (25 °C) in water (b and d, respectively). Peaks: 1, poly(NIPAM-*co*-MBC-AA); 2, poly(NIPAM-*co*-MBC-AE); and 3, fluorescent compounds cleaved from poly(NIPAM-*co*-MBC-AE). The fluorescence intensity at 470 nm was monitored with excitation at 345 nm.

phenolic hydroxyl group; and (c) it contains only one fluorophore, which reduces the possibility of undesirable interactions with bio-relevant molecules when applied to probe cellular temperatures. In summary, the new fluorescent monomer **MBC-AA** is expected to aid in the development of novel functional polymeric sensors, especially because **MBC-AA** is highly robust and highly sensitive to environmental changes. In the near future, new stimulus-responsive polymeric materials will be created through the application of **MBC-AA**. Our research group is now pursuing this research direction.

Acknowledgements

molecule (2.7% °C^{-1}),[24] GFP (1.3% °C^{-1}),[25] and others (1.7–3.9% °C^{-1})[26] (see Table S1† for a detailed comparison). The high sensitivity of poly(NIPAM-*co*-MBC-AA) clearly originated from the environment-sensitive **MBC-AA** units. Furthermore, poly(NIPAM-*co*-MBC-AA) has several advantages in ratiometric temperature sensing because (a) it requires only a single excitation to exhibit fluorescence at two different wavelengths; (b) the **MBC-AA** unit is pH insensitive because of the lack of a pH-sensitive structure, such as an amino group or a
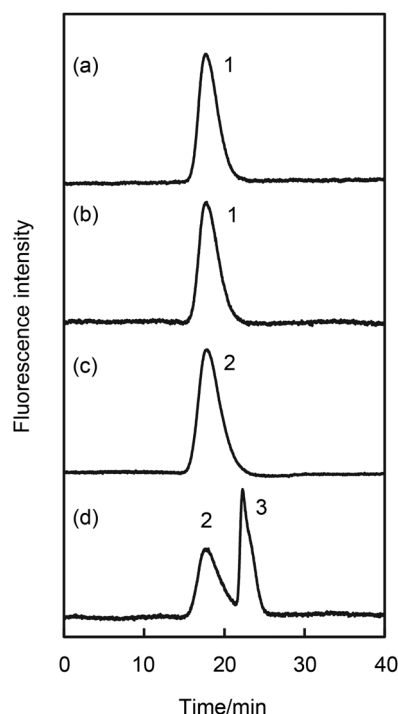
1244 | *Photochem. Photobiol. Sci.*, 2016, **15**, 1239–1246

This journal is © The Royal Society of Chemistry and Owner Societies 2016

Notes and references

1 (a) K. J. Shea, G. J. Stoddard, D. M. Shavelle, F. Wakui and R. M. Choate, Synthesis and characterization of highly cross-linked polyacrylamides and polymethacrylamides. A new class of macroporous polyamides, *Macromolecules*, 1990, **23**, 4497–4507; (b) Y. Hattori, K. Nagase, J. Kobayashi, A. Kikuchi, Y. Akiyama, H. Kanazawa and T. Okano, Hydration of poly(N-isopropylacrylamide) brushes on micro-silica beads measured by a fluorescent probe, *Chem. Phys. Lett.*, 2010, **491**, 193–198.

2 (a) Z. Yang, J. Cao, Y. He, J. H. Yang, T. Kim, X. Peng and J. S. Kim, Macro-/micro-environment-sensitive chemo-sensing and biological imaging, *Chem. Soc. Rev.*, 2014, **43**, 4563–4601; (b) J. Hu and S. Liu, Responsive polymers for detection and sensing applications: current status and future developments, *Macromolecules*, 2010, **43**, 8315–8330.

3 A. Yamada, Y. Hiruta, J. Wang, E. Ayano and H. Kanazawa, Design of environmentally responsive fluorescent polymer probes for cellular imaging, *Biomacromolecules*, 2015, **16**, 2356–2362.

4 (a) T. Wu, G. Zou, J. Hu and S. Liu, Fabrication of photo-switchable and thermotunable multicolor fluorescent hybrid silica nanoparticles coated with dye-labeled poly(N-isopropylacrylamide) brushes, *Chem. Mater.*, 2009, **21**, 3788–3798; (b) C. Li, Y. Zhang, J. Hu, J. Cheng and S. Liu, Reversible three-state switching of multicolor fluorescence emission by multiple stimuli modulated FRET processes within thermoresponsive polymeric micelles, *Angew. Chem., Int. Ed.*, 2010, **49**, 5120–5124; (c) Y. Wu, H. Hu, J. Hu, T. Liu, G. Zhang and S. Liu, Thermo- and light-regulated formation and disintegration of double hydrophilic block copolymer assemblies with tunable fluorescence emissions, *Langmuir*, 2013, **29**, 3711–3720.

5 (a) S. Uchiyama, Y. Matsumura, A. P. de Silva and K. Iwai, Fluorescent molecular thermometers based on polymers showing temperature-induced phase transitions and labeled with polarity-responsive benzofurazans, *Anal. Chem.*, 2003, **75**, 5926–5935; (b) S. Uchiyama, Y. Matsumura, A. P. de Silva and K. Iwai, Modulation of the sensitive temperature range of fluorescent molecular thermometers based on thermoresponsive polymers, *Anal. Chem.*, 2004, **76**, 1793–1798; (c) S. Uchiyama, N. Kawai, A. P. de Silva and K. Iwai, Fluorescent polymeric AND logic gate with temperature and pH as inputs, *J. Am. Chem. Soc.*, 2004, **126**, 3032–3033; (d) C. Gota, S. Uchiyama and T. Ohwada, Accurate fluorescent polymeric thermometers containing an ionic component, *Analyst*, 2007, **132**, 121–126; (e) C. Gota, S. Uchiyama, T. Yoshihara, S. Tobita and T. Ohwada, Temperature-dependent fluorescence lifetime of a fluorescent polymeric thermometer, poly(N-isopropyl-acrylamide), labeled by polarity and hydrogen bonding sensitive 4-sulfamoyl-7-aminobenzofurazan, *J. Phys. Chem. B*, 2008, **112**, 2829–2836.

6 (a) C. Gota, K. Okabe, T. Funatsu, Y. Harada and S. Uchiyama, Hydrophilic fluorescent nanogel thermometer for intracellular thermometry, *J. Am. Chem. Soc.*, 2009, **131**, 2766–2767; (b) K. Okabe, N. Inada, C. Gota, Y. Harada, T. Funatsu and S. Uchiyama, Intracellular temperature mapping with a fluorescent polymeric thermometer and fluorescence lifetime imaging microscopy, *Nat. Commun.*, 2012, **3**, 705; (c) T. Tsuji, S. Yoshida, A. Yoshida and S. Uchiyama, Cationic fluorescent polymeric thermometers with the ability to enter yeast and mammalian cells for practical intracellular temperature measurements, *Anal. Chem.*, 2013, **85**, 9815–9823; (d) T. Hayashi, N. Fukuda, S. Uchiyama and N. Inada, A cell-permeable fluorescent polymeric thermometer for intracellular temperature mapping in mammalian cell lines, *PLoS One*, 2015, **10**, e0117677; (e) S. Uchiyama, T. Tsuji, K. Ikado, A. Yoshida, K. Kawamoto, T. Hayashi and N. Inada, A cationic fluorescent polymeric thermometer for the ratiometric sensing of intracellular temperature, *Analyst*, 2015, **140**, 4498–4506.

7 S. Inal, J. D. Kölsch, F. Sellrie, J. A. Schenk, E. Wischerhoff, A. Laschewsky and D. Neher, A water soluble fluorescent polymer as a dual colour sensor for temperature and a specific protein, *J. Mater. Chem. B*, 2013, **1**, 6373–6381.

8 S. Inal, J. D. Kölsch, L. Chiappisi, D. Janietz, M. Gradzielski, A. Laschewsky and D. Neher, Structure-related differences in the temperature-regulated fluorescence response of LCST type polymers, *J. Mater. Chem. C*, 2013, **1**, 6603–6612.

9 (a) N. Inada and S. Uchiyama, Methods and benefits of imaging the temperature distribution inside living cells, *Imaging Med.*, 2013, **5**, 303–305; (b) S. Uchiyama and N. Inada, Cellular thermometry, in *Thermometry at the Nanoscale: Techniques and Selected Applications*, ed. L. D. Carlos and F. Palacio, Royal Society of Chemistry, Cambridge, 2016, pp. 355–382.

10 J. Yin, C. Li, D. Wang and S. Liu, FRET-derived ratiometric fluorescent K$^+$ sensors fabricated from thermoresponsive poly(N-isopropylacrylamide) microgels labeled with crown ether moieties, *J. Phys. Chem. B*, 2010, **114**, 12213–12220.

11 M. Onoda, S. Uchiyama and T. Ohwada, Fluorogenic ion sensing system working in water, based on stimulus-responsive copolymers incorporating a polarity-sensitive fluorophore, *Macromolecules*, 2007, **40**, 9651–9657.

12 Y. Yoon, P. J. Lee, S. Kurilova and W. Cho, *In situ* quantitative imaging of cellular lipids using molecular sensors, *Nat. Chem.*, 2011, **3**, 868–874.

13 S.-L. Liu, R. Sheng, M. J. O'Connor, Y. Cui, Y. Yoon, S. Kurilova, D. Lee and W. Cho, Simultaneous in situ quantification of two cellular lipid pools using orthogonal fluorescent sensors, *Angew. Chem., Int. Ed.*, 2014, **53**, 14387–14391.

14 S. Uchiyama, K. Takehira, T. Yoshihara, S. Tobita and T. Ohwada, Environment-sensitive fluorophore emitting in protic environments, *Org. Lett.*, 2006, **8**, 5869–5872.

15 (a) H. G. Schild, Poly(N-isopropylacrylamide): experiment, theory and application, *Prog. Polym. Sci.*, 1992, **17**, 163–249; (b) A. Halperin, M. Kröger and F. M. Winnik,

This journal is © The Royal Society of Chemistry and Owner Societies 2016

Photochem. Photobiol. Sci., 2016, **15**, 1239–1246 | **1245**

Poly(*N*-isopropylacrylamide) phase diagrams: fifty years of research, *Angew. Chem., Int. Ed.*, 2015, **54**, 15342–15367.

16 M. J. Kamlet, J.-L. M. Abboud, M. H. Abraham and R. W. Taft, Linear solvation energy relationships. 23. A comprehensive collection of the solvatochromic parameters, π*, α, and β, and some methods for simplifying the generalized solvatochromic equation, *J. Org. Chem.*, 1983, **48**, 2877–2887.

17 (*a*) A. A. Maryott and E. R. Smith, *Table of Dielectric Constants of Pure Liquids*, U. S. Govt. Print. Off., Washington, 1951; (*b*) T. Shedlovsky and R. L. Kay, The ionization constant of acetic acid in water-methanol mixtures at 25° from conductance measurements, *J. Phys. Chem.*, 1956, **60**, 151–155; (*c*) Y. Tanaka, Y. F. Xiao and S. Matsuo, Relative permittivity of fluoroalcohols at temperature from 293 to 323 K and pressures up to 50 MPa, *Fluid Phase Equilib.*, 2000, **170**, 139–149.

18 (*a*) J. R. Lakowicz, in *Principles of Fluorescence Spectroscopy*, Springer, New York, 3rd edn, 2006, p. 205; (*b*) B. Valeur and M. N. Berberan-Santos, in *Molecular Fluorescence: Principles and Applications*, Wiley, Weinheim, 2nd edn, 2012, p. 379.

19 A. Kobayashi, K. Takehira, T. Yoshihara, S. Uchiyama and S. Tobita, Remarkable fluorescence enhancement of benzo[*g*]chromen-2-ones induced by hydrogen-bonding interactions with protic solvents, *Photochem. Photobiol. Sci.*, 2012, **11**, 1368–1376.

20 (*a*) R. Englman and J. Jortner, The energy gap law for non-radiative decay in large molecules, *J. Lumin.*, 1970, **1–2**, 134–142; (*b*) N. J. Turro, in *Modern Molecular Photochemistry*, University Science Books, Sausalito, 1991, p. 183.

21 (*a*) C. Pietsch, A. Vollrath, R. Hoogenboom and U. S. Schubert, A fluorescent thermometer based on a pyrene-labeled thermoresponsive polymer, *Sensors*, 2010, **10**, 7979–7990; (*b*) C.-Y. Chen and S.-T. Chen, A PNIPAM-based fluorescent nanothermometer with ratiometric readout, *Chem. Commun.*, 2011, **47**, 994–996; (*c*) J. Hu, L. Dai and S. Liu, Analyte-reactive amphiphilic thermoresponsive diblock copolymer micelles-based multifunctional ratiometric fluorescent chemosensors, *Macromolecules*, 2011, **44**, 4699–4710; (*d*) J. Hu, X. Zhang, D. Wang, X. Hu, T. Liu, G. Zhang and S. Liu, Ultrasensitive ratiometric fluorescent pH and temperature probes constructed from dye-labeled thermoresponsive double hydrophilic block copolymers, *J. Mater. Chem.*, 2011, **21**, 19030–19038; (*e*) J. Liu, X. Guo, R. Hu, J. Xu, S. Wang, S. Li, Y. Li and G. Yang, Intracellular fluorescent temperature probe based on triarylboron substituted poly *N*-isopropylacrylamide and energy transfer, *Anal. Chem.*, 2015, **87**, 3694–3698; (*f*) J. Qiao, Y.-H. Hwang, C.-F. Chen, L. Qi, P. Dong, X.-Y. Mu and D.-P. Kim, Ratiometric fluorescent polymeric thermometer for thermogenesis investigation in living cells, *Anal. Chem.*, 2015, **87**, 10535–10541; (*g*) F. Pinaud, R. Millereux, P. Vialar-Trarieux, B. Catargi, S. Pinet, I. Gosse, N. Sojic and V. Ravaine, Differential photoluminescent and electrochemiluminescent behavior

for resonance energy transfer processes in thermoresponsive microgels, *J. Phys. Chem. B*, 2015, **119**, 12954–12961.

22 (*a*) Y. Takei, S. Arai, A. Murata, M. Takabayashi, K. Oyama, S. Ishiwata, S. Takeoka and M. Suzuki, A nanoparticle-based ratiometric and self-calibrated fluorescent thermometer for single living cells, *ACS Nano*, 2014, **8**, 198–206; (*b*) S. Arai, Ferdinandus, S. Takeoka, S. Ishiwata, H. Sato and M. Suzuki, Micro-thermography in millimeter-scale animals by using orally-dosed fluorescent nanoparticle thermosensors, *Analyst*, 2015, **140**, 7534–7539; (*c*) R. Piñol, C. D. S. Brites, R. Bustamante, A. Martínez, N. J. O. Silva, J. L. Murillo, R. Cases, J. Carrey, C. Estepa, C. Sosa, F. Palacio, L. D. Carlos and A. Millán, Joining time-resolved thermometry and magnetic-induced heating in a single nanoparticle unveils intriguing thermal properties, *ACS Nano*, 2015, **9**, 3134–3142.

23 (*a*) F. Vetrone, R. Naccache, A. Zamarrón, A. J. de la Fuente, F. Sanz-Rodríguez, L. M. Maestro, E. M. Rodriguez, D. Jaque, J. G. Solé and J. A. Capobianco, Temperature sensing using fluorescent nanothermometers, *ACS Nano*, 2010, **4**, 3254–3258; (*b*) E. J. McLaurin, V. A. Vlaskin and D. R. Gamelin, Water-soluble dual-emitting nanocrystals for ratiometric optical thermometry, *J. Am. Chem. Soc.*, 2011, **133**, 14978–14980; (*c*) N.-N. Dong, M. Pedroni, F. Piccinelli, G. Conti, A. Sbarbati, J. E. Ramírez-Hernández, L. M. Maestro, M. C. Iglesias-de la Cruz, F. Sanz-Rodriguez, A. Juarranz, F. Chen, F. Vetrone, J. A. Capobianco, J. G. Solé, M. Bettinelli, D. Jaque and A. Speghini, NIR-to-NIR two-photon excited CaF₂: Tm³⁺, Yb³⁺ nanoparticles: multifunctional nanoprobes for highly penetrating fluorescence bio-imaging, *ACS Nano*, 2011, **5**, 8665–8671; (*d*) A. Sedlmeier, D. E. Achatz, L. H. Fischer, H. H. Gorris and O. S. Wolfbeis, Photon upconverting nanoparticles for luminescent sensing of temperature, *Nanoscale*, 2012, **4**, 7090–7096; (*e*) R. Tanimoto, T. Hiraiwa, Y. Nakai, Y. Shindo, K. Oka, N. Hiroi and A. Funahashi, Detection of temperature difference in neuronal cells, *Sci. Rep.*, 2016, **6**, 22071.

24 M. Homma, Y. Takei, A. Murata, T. Inoue and S. Takeoka, A ratiometric fluorescent molecular probe for visualization of mitochondrial temperature in living cells, *Chem. Commun.*, 2015, **51**, 6194–6197.

25 S. Kiyonaka, T. Kajimoto, R. Sakaguchi, D. Shinmi, M. Omatsu-Kanbe, H. Matsuura, H. Imamura, T. Yoshizaki, I. Hamachi, T. Morii and Y. Mori, Genetically encoded fluorescent thermosensors visualize subcellular thermoregulation in living cells, *Nat. Methods*, 2013, **10**, 1232–1238.

26 (*a*) H.-S. Peng, S.-H. Huang and O. S. Wolfbeis, Ratiometric fluorescent nanoparticles for sensing temperature, *J. Nanopart. Res.*, 2010, **12**, 2729–2733; (*b*) F. Ye, C. Wu, Y. Jin, Y.-H. Chan, X. Zhang and D. T. Chiu, Ratiometric temperature sensing with semiconducting polymer dots, *J. Am. Chem. Soc.*, 2011, **133**, 8146–8149; (*c*) A. E. Albers, E. M. Chan, P. M. McBride, C. M. Ajo-Franklin, B. E. Cohen and B. A. Helms, Dual-emitting quantum dot/quantum rod-based nanothermometers with enhanced response and sensitivity in live cells, *J. Am. Chem. Soc.*, 2012, **134**, 9565–9568.

1246 | *Photochem. Photobiol. Sci.*, 2016, **15**, 1239–1246

This journal is © The Royal Society of Chemistry and Owner Societies 2016